

Iterative Hard Thresholding for Model Selection in Genome-Wide Association Studies

Kevin L. Keys^{1*},
Gary K. Chen²,
and Kenneth Lange^{1,3}

¹ Department of Biomathematics, University of California, Los Angeles, CA 90095

² Division of Biostatistics, University of Southern California, Los Angeles, CA 90089

³ Departments of Human Genetics and Statistics, University of California, Los Angeles, CA 90095

*To whom correspondence should be addressed.

January 21, 2019

Abstract

A genome-wide association study (GWAS) correlates marker variation with trait variation in a sample of individuals. Each study subject is genotyped at a multitude of SNPs (single nucleotide polymorphisms) spanning the genome. Here we assume that subjects are unrelated and collected at random and that trait values are normally distributed or transformed to normality. Over the past decade, researchers have been remarkably successful in applying GWAS analysis to hundreds of traits. The massive amount of data produced in these studies present unique computational challenges. Penalized regression with LASSO or MCP penalties is capable of selecting a handful of associated SNPs from millions of potential SNPs. Unfortunately, model selection can be corrupted by false positives and false negatives, obscuring the genetic underpinning of a trait. This paper introduces the iterative hard thresholding (IHT) algorithm to the GWAS analysis of continuous traits. Our parallel implementation of IHT accommodates SNP genotype compression and exploits multiple CPU cores and graphics processing units (GPUs). This allows statistical geneticists to leverage commodity desktop computers in GWAS analysis and to avoid supercomputing. We evaluate IHT performance on both simulated and real GWAS data and conclude that it reduces false positive and false negative rates while remaining competitive in computational time with penalized regression. Source code is freely available at <https://github.com/klkeys/IHT.jl>.

1 Introduction

A genome-wide association study (GWAS) examines the influence of a multitude of genetic variants on a given trait. Over the past decade, GWAS has benefitted from technological advances in dense genotyping arrays, high-throughput sequencing, and more powerful computing resources. Yet researchers still struggle to find the genetic variants that account for the missing heritability of many traits. It is now common for consortia studying a complex trait such as height to pool results across multiple sites and countries. Meta-analyses have discovered hundreds of statistically significant SNPs, each of which explains a small fraction of the total heritability. A drawback of GWAS meta-analysis is that it relies on univariate regression rather than on more informative multivariate regression (Yang *et al.*, 2010). Because the number of SNPs (predictors) in a GWAS vastly exceeds the number of study subjects (observations), statistical ge-

neticists have resorted to machine learning techniques such as penalized regression (Lange *et al.*, 2014) for model selection.

In the statistical setting of n subjects and p predictors with $n \ll p$, penalized regression estimates a sparse statistical model $\beta \in \mathbb{R}^p$ by minimizing a penalized loss $f(\beta) + \lambda p(\beta)$, where $f(\beta)$ is a convex loss, $p(\beta)$ is a suitable penalty, and λ is a tuning constant controlling the sparsity of β . The most popular and mature sparse regression tool is LASSO (ℓ_1) regression. It is known that LASSO parameter estimates are biased towards zero (Hastie *et al.*, 2009), often severely so, as a consequence of shrinkage. Shrinkage in itself is not terribly harmful, but LASSO regression lets too many false positives enter a model. Since GWAS is often followed by expensive biological validation studies, there is value in reducing false positive rates. In view of the side effects of shrinkage, Zhang (2010) recommends the minimax concave penalty (MCP) as an alternative to the ℓ_1 penalty. Other non-convex penalties exist, but MCP is probably the simplest to implement. MCP also has provable convergence guarantees. In contrast to the LASSO, which admits too many false positives, MCP tends to allow too few predictors to enter a model. Thus, its false negative rate is too high. Our subsequent numerical examples confirm these tendencies.

Surprisingly few software packages implement efficient penalized regression algorithms for GWAS. The R packages `glmnet` and `ncvreg` are ideal candidates given their ease of use, maturity of development, and wide acceptance. The former implements LASSO-penalized regression (Friedman *et al.*, 2010; Lange, 2010; Tibshirani, 1996), while the latter implements both LASSO- and MCP-penalized regression (Breheny and Huang, 2011; Zhang, 2010). Both packages provide excellent functionality for moderately sized problems. However, their scalability to GWAS is encumbered by R’s poor memory management. In fact, analysis on a typical workstation is limited to at most a handful of chromosomes. Larger problems must appeal to cluster or cloud computing. Neither `glmnet` nor `ncvreg` natively support the compressed PLINK binary genotype file (BED file) format typically used to efficiently store and distribute GWAS data (Purcell *et al.*, 2007). Scalable implementations of LASSO for GWAS with PLINK files appear in the packages `Mendel`, `gpu-lasso`, `SparSNP`, and the beta version of PLINK 1.9 (Abraham *et al.*, 2012; Chang *et al.*, 2015; Chen, 2012; Lange *et al.*, 2013; Wu and Lange, 2008). All of these packages include parallel computing capabilities for large GWAS datasets. `Mendel`, `gpu-lasso`, and PLINK 1.9 beta have multicore acceleration capabilities, while `SparSNP` can be run on compute clusters. To our knowledge, only `Mendel` supports MCP regression with PLINK files.

As an alternative to penalized regression, one can tackle sparsity directly through projection onto sparsity sets (Blumensath, 2012; Blumensath and Davies, 2008, 2009, 2010). Iterative hard thresholding (IHT) minimizes a loss function $f(\beta)$ subject to the sparsity constraint $\|\beta\|_0 \leq k$, where the ℓ_0 “norm” $\|\beta\|_0$ counts the number of nonzero entries of the parameter vector β . The integer k serves as a tuning constant analogous to λ in LASSO and MCP regression. IHT can be viewed as a version of *projected gradient descent* tailored to sparse regression. Similar algorithms treated in the signal processing literature include hard thresholding pursuit (Bahmani *et al.*, 2013; Foucart, 2011; Yuan *et al.*, 2014), matching pursuit (Mallat and Zhang, 1993; Needell and Tropp, 2009; Tropp and Gilbert, 2007), and subspace pursuit (Dai and Milenkovic, 2009). Since these algorithms rely solely on gradients, they avoid computing and inverting large Hessian matrices and hence scale well to large datasets.

In addition, our implementation of IHT addresses some of the specific concerns of GWAS. First, it accommodates genotype compression when genotypes are presented in compressed PLINK format. Second, our version of IHT allows the user to choose the sparsity level k of a model. In contrast, LASSO and MCP penalized regression must choose the model size indirectly by adjusting the tuning constant λ to match a given k . Third, our version of IHT is implemented in the package `IHT.jl` in the Julia programming language. Julia is available on a variety of hardware platforms. It also encourages prudent control of memory, exploits all available CPU cores, and interfaces with massively parallel graphics processing unit (GPU) devices. Finally, our version of IHT performs more parsimonious model selection than either LASSO or MCP penalized regression. All of these advantages can be realized on a modern desktop computer. Although our current IHT implementation is limited to ordinary linear least squares, the literature suggests that logistic regression is ultimately within reach (Bahmani *et al.*, 2013;

Yuan *et al.*, 2014).

At this juncture, we stress that our focus is on parameter estimation and model selection. IHT currently lacks a coherent inference framework for constructing valid postselective confidence intervals and P -values. In contrast, a valid postselective inference theory for the LASSO (Lockhart *et al.*, 2014; Taylor and Tibshirani, 2015; Lee *et al.*, 2016) is supported by the R package `selectiveInference`. Because this package lacks PLINK file support and parallel capabilities, its scalability to GWAS is unclear.

Before moving onto the rest of the paper, let us sketch its main contents. Section 2 describes penalized regression and the IHT algorithm. We dwell in particular on the tactics necessary for parallelization. Section 3 records our numerical experiments. The performance of IHT and competing algorithms is evaluated by several metrics: computation time, false positive rates, false negative rates, and prediction error. The sparsity level k for a given dataset is chosen by cross-validation on both real and simulated genetic data. Our discussion in Section 4 summarizes results, limitations, and precautions.

2 Methods

2.1 Penalized regression

Consider a statistical design matrix $\mathbf{X} \in \mathbb{R}^{n \times p}$, a noisy n -dimensional response \mathbf{y} , and a sparse statistical vector $\boldsymbol{\beta}$ of regression coefficients. When \mathbf{y} represents a continuous phenotype, then the residual sum of squares

$$f(\boldsymbol{\beta}) = \frac{1}{2} \|\mathbf{y} - \mathbf{X}\boldsymbol{\beta}\|_2^2 \quad (1)$$

is a reasonable choice for the loss $f(\boldsymbol{\beta})$. LASSO penalized regression imposes the convex ℓ_1 penalty $p_\lambda(\boldsymbol{\beta}) = \lambda \|\boldsymbol{\beta}\|_1 = \lambda \sum_{i=1}^p |\beta_i|$. In most applications the intercept contribution $|\beta_1|$ is omitted from the penalty. Various approaches exist to minimize the objective $f(\boldsymbol{\beta}) + \lambda \|\boldsymbol{\beta}\|_1$, including least angle regression (LARS) (Efron *et al.*, 2004), cyclic coordinate descent (Friedman *et al.*, 2007; Wu *et al.*, 2009; Wu and Lange, 2008), and the fast iterative shrinkage and thresholding algorithm (FISTA) (Beck and Teboulle, 2009). The ℓ_1 norm penalty induces both sparsity and shrinkage. Shrinkage per se is not an issue because selected parameters can be re-estimated with both the non-selected parameters and the penalty removed. However, the severe shrinkage induced by the LASSO inflates false negative rates since spurious predictors enter the model to absorb the unexplained variance left by the shrinkage imposed on the true predictors.

The MCP alternative to LASSO takes $p_{\lambda, \gamma}(\boldsymbol{\beta}) = \sum_{i=1}^p q(|\beta_i|)$ with

$$q(\beta_i) = \begin{cases} \lambda \beta_i - \beta_i^2 / (2\gamma) & 0 \leq \beta_i \leq \gamma\lambda \\ \gamma\lambda^2 / 2 & \beta_i > \gamma\lambda \end{cases}$$

$$q'(\beta_i) = \begin{cases} \lambda - \beta_i / \gamma & 0 \leq \beta_i < \gamma\lambda \\ 0 & \beta_i > \gamma\lambda \end{cases} \quad (2)$$

for positive tuning constants λ and γ . The MCP penalty (2) attenuates penalization for large parameter values. Indeed, beyond $\beta_i = \gamma\lambda$, MCP does not subject β_i to further shrinkage pressure. Relaxing penalization of large entries of $\boldsymbol{\beta}$ ameliorates LASSO's shrinkage. If one majorizes the MCP function $q(\beta_i)$ by a scaled absolute value function, then cyclic coordinate descent parameter updates resemble LASSO updates (Jiang and Huang, 2011).

2.2 Projection algorithms

The ℓ_1 penalty is the smallest convex relaxation of the ℓ_0 penalty. As mentioned earlier, one can obtain sparsity without shrinkage by directly minimizing $f(\boldsymbol{\beta})$ subject to $\|\boldsymbol{\beta}\|_0 \leq k$. This subset selection

problem is known to be NP-hard (Golub *et al.*, 1976; Natarajan, 1995). IHT *approximates* the solution to the subset selection problem by taking the projected gradient steps

$$\beta^{m+1} = P_{S_k}[\beta^m - \mu \nabla f(\beta^m)], \quad (3)$$

where μ denotes the step size of the algorithm, and $P_{S_k}(\beta)$ denotes the projection of β onto the sparsity set S_k where at most k components of a vector are nonzero. Projection is accomplished by setting all but the k largest components of β in magnitude equal to 0. For sufficiently small μ , the projected gradient update (3) is guaranteed to reduce the loss, but it forfeits stronger convergence properties because S_k is nonconvex.

Recent research has derived guarantees of stable convergence and model recovery for nonconvex projected gradient schemes under a few ideal assumptions. Conditions for convergence include *restricted strong convexity* (RSC) (Dobson and Barnett, 2008; Loh and Wainwright, 2013) and *restricted strong smoothness* (RSS) (Agarwal *et al.*, 2012; Jain *et al.*, 2014). Together RSC and RSS place local bounds on the curvature of the loss function. One can show that if f satisfies RSC and RSS, then IHT will converge to a k -sparse minimizer β of f provided that the extreme eigenvalues of the Hessian matrix $\nabla^2 f(\beta^*)$ are bounded for any k -sparse approximation β^* near β . Conditions for sparse recovery include the *restricted isometry property* (RIP) (Candés *et al.*, 2006) and *mutual coherence* (Tropp, 2006). RIP and mutual coherence together require that \mathbf{X} (or its normalized variant) behave like an orthonormal matrix whose columns are not strongly correlated with each other. In a GWAS context, these results imply that IHT will recover the true model provided that the SNP markers in \mathbf{X} are not in strong linkage disequilibrium with each other.

2.3 Calculating step sizes

Computing a reasonable step size μ is important for ensuring stable descent in projected gradient schemes. For the case of least squares regression, our implementation of IHT uses the “normalized” update of Blumensath and Davies (Blumensath and Davies, 2010). At each iteration m , this amounts to employing the step size

$$\mu_m = \frac{\|\beta^m\|_2^2}{\|\mathbf{X}\beta^m\|_2^2}.$$

Convergence is guaranteed provided that $\mu < \omega$, where

$$\omega = (1 - c) \frac{\|\beta^{m+1} - \beta^m\|_2^2}{\|\mathbf{X}(\beta^{m+1} - \beta^m)\|_2^2} \quad (4)$$

for some constant $0 < c \ll 1$. One can interpret ω as the normed ratio of the difference between successive iterates versus the difference between successive estimated responses.

2.4 Bandwidth optimizations

Analysis of large GWAS datasets requires intelligent handling of memory and read/write operations. Our software reads datasets in PLINK binary format, which stores each genotype in two bits. The PLINK compression protocol attains 32x compression by reducing 64-bit floats to 2-bit integers. Although PLINK compression facilitates storage and transport of data, it complicates linear algebra operations. On small datasets, we store the design matrix \mathbf{X} in floating point. On large datasets, we store both a compressed \mathbf{X} and a compressed transpose \mathbf{X}^T . The transpose \mathbf{X}^T is used to compute the gradient $\nabla f(\beta) = -\mathbf{X}^T(\mathbf{y} - \mathbf{X}\beta)$, while \mathbf{X} is used to compute the predicted response $\mathbf{X}\beta$. The counterintuitive tactic of storing both \mathbf{X} and \mathbf{X}^T roughly doubles the memory required to store genotypes. However, it facilitates accessing all data in column-major and unit stride order, thereby ensuring that all linear algebra operations maintain full memory caches.

Good statistical practice dictates standardizing all predictors; otherwise, parameters are penalized nonuniformly. Standardizing nongenetic covariates is trivial. However, one cannot store standardized genotypes in PLINK binary format. The remedy is to precompute and cache vectors \mathbf{u} and \mathbf{v} containing the mean and precision, respectively, of each of the p SNPs. The product $\mathbf{X}_{\text{st}}\boldsymbol{\beta}$ invoking the standardized predictor matrix \mathbf{X}_{st} can be recovered via the formula

$$\mathbf{X}_{\text{st}}\boldsymbol{\beta} = \mathbf{X} \text{diag}(\mathbf{v})\boldsymbol{\beta} - \mathbf{1}\mathbf{u}^T \text{diag}(\mathbf{v})\boldsymbol{\beta},$$

where $\mathbf{1}$ is an n -vector of ones and $\text{diag}(\mathbf{v})$ is a diagonal matrix with \mathbf{v} on the main diagonal. Thus, there is no need to explicitly store \mathbf{X}_{st} .

On-the-fly standardization is a costly operation and must be employed judiciously. For example, to calculate $\mathbf{X}\boldsymbol{\beta}$ we exploit the structural sparsity of $\boldsymbol{\beta}$ by only decompressing and standardizing the submatrix \mathbf{X}_k of \mathbf{X} corresponding to the k nonzero values in $\boldsymbol{\beta}$. We then use \mathbf{X}_k for parameter updates until we observe a change in the support of $\boldsymbol{\beta}$. Unfortunately, calculation of the gradient $\nabla f(\boldsymbol{\beta})$ offers no such optimization because it requires a fully decompressed matrix \mathbf{X}^T . Since we cannot store all $n \times p$ standardized genotypes in floating point format, the best that we can achieve is standardization on-the-fly every time we update the gradient.

2.5 Parallelization

Our implementation of IHT for PLINK files relies on two parallel computing schemes. First, we make heavy use of multicore computing with shared memory arrays to distribute computations over all cores in a CPU. For example, suppose that we wish to compute in parallel the column means of \mathbf{X} stored in a shared memory array. The mean of each column is independent of the others, so the computations distribute naturally across multiple cores. If a CPU contains four available cores, then we enlist four cores for our computations, one master and three workers. Each worker can see the entirety of \mathbf{X} but only works on a subset of its columns. The workers compute the column means for the three chunks of \mathbf{X} in parallel. Columnwise operations, vector arithmetic, and matrix-vector operations fit within this paradigm.

The two most expensive operations are the matrix-vector multiplications $\mathbf{X}\boldsymbol{\beta}$ and $\mathbf{X}^T(\mathbf{y} - \mathbf{X}\boldsymbol{\beta})$. We previously discussed intelligent computation of $\mathbf{X}\boldsymbol{\beta}$ via $\mathbf{X}_k\boldsymbol{\beta}_k$. Dense multithreaded linear algebra libraries such as BLAS facilitate efficient computation of $\mathbf{X}_k\boldsymbol{\beta}_k$. Consequently, we obtain $\mathbf{X}\boldsymbol{\beta}$ in $\mathcal{O}(nk)$ total operations. In contrast, the gradient $\nabla f(\boldsymbol{\beta}) = -\mathbf{X}^T(\mathbf{y} - \mathbf{X}\boldsymbol{\beta})$ in the update (3) requires a completely dense matrix-vector multiplication with a run-time complexity of $\mathcal{O}(np)$. We could lighten the computational burden by cluster computing, but communication between the different nodes then takes excessive time.

A reasonable alternative for acceleration is to calculate the gradient on a GPU running OpenCL kernel code. An optimal GPU implementation must minimize memory transactions between the device GPU and the host CPU. Our solution is to push the compressed PLINK matrix \mathbf{X} and its column means and precisions onto the device at the start of the algorithm. We also cache device buffers for the residuals and the gradient. Whenever we calculate the gradient, we compute the n residuals on the host and then push the residuals onto the device. At this stage, the device executes two kernels. The first kernel initializes many workgroups of threads and distributes a block of $\mathbf{X}^T(\mathbf{y} - \mathbf{X}\boldsymbol{\beta})$ to each workgroup. Each thread handles the decompression, standardization, and computation of one component of \mathbf{X} with the residuals. The second kernel reduces across all thread blocks and returns the p -dimensional gradient. Finally, the host pulls the p -dimensional gradient from the device. Thus, after the initialization of the data, our GPU implementation only requires the host and device to exchange $p+n$ floating point numbers per iteration.

2.6 Selecting the best model

Given a regularization path computed by the IHT, the obvious way to choose the best model along the path is to resort to q -fold cross-validation with mean squared error (MSE) as a selection criterion. For

a path of user-supplied model sizes k_1, k_2, \dots, k_r , our implementation of IHT fits the entire path on the $q - 1$ training partitions. We then view the q th partition as a testing set and compute its mean squared error (MSE). Finally, we determine the model size k with minimum MSE and refit the data subject to $\|\beta\|_0 \leq k$.

3 Results

We tested our IHT implementation on data from the Northern Finland Birth Cohort 1966 (NFBC1966) (Sabatti *et al.*, 2009). These data contain several biometric phenotypes for 5402 patients genotyped at 370,404 SNPs. We imputed the missing genotypes in \mathbf{X} with Mendel (Ayers and Lange, 2008) and performed quality control with PLINK 1.9 beta (Chang *et al.*, 2015). Our numerical experiments include both simulated and measured phenotypes. For our simulated phenotype, we benchmarked the model recovery and predictive performance of our software against `glmnet` v2.0.5 and `ncvreg` v3.6.0 (Breheny and Huang, 2011; Friedman *et al.*, 2010) in R v3.2.4. Sections 3.2 and 3.3 include as non-genetic covariates the SEXOCPG factor, which we calculated per Sabatti *et al.*, and the first two principal components of \mathbf{X} , which we calculated with PLINK 1.9. All numerical experiments were run on a single compute node equipped with four 6-core 2.67Ghz Intel Xeon CPUs and two NVIDIA Tesla C2050 GPUs, each with 6Gb of memory. To simulate performance on a workstation, the experiment only used one GPU and one CPU. The compute environment was 64-bit Julia v0.5.0 with the corresponding OpenBLAS library and LLVM v3.3 compiler.

3.1 Simulation

The goal of our first numerical experiment was to demonstrate the superior model selection performance of IHT versus LASSO and MCP. Here we used only the matrix \mathbf{X}_{chr1} of 24,663 SNPs from chromosome 1 of the NFBC1966 dataset. This matrix is sufficiently small to render PLINK compression and GPU acceleration unnecessary. \mathbf{X}_{chr1} uses the 5289 cases with observed BMI. Note that this number is larger than what we will use in Sections 3.2 and 3.3; no exclusion criteria were applied here since the phenotype was simulated. We standardized observed genotype dosages and then set any unobserved dosages to 0. We simulated β_{true} for true model sizes $k_{\text{true}} \in \{100, 200, 300\}$ and effect sizes drawn from the normal distribution $N(0, 0.01)$. The simulated phenotypes were then formed as $\mathbf{y}_{\text{true}} = \mathbf{X}_{\text{chr1}}\beta_{\text{true}} + \epsilon$, with each $\epsilon_i \sim N(0, 0.01)$. To assess predictive performance, we separated 289 individuals as a validation set and used the remaining 5000 individuals for 5-fold cross-validation. We generated 10 different models for each k_{true} . For each replicate, we ran regularization paths of 100 model sizes $k_0, k_0 + 2, \dots, k_{\text{true}}, k_{\text{true}} + 2, \dots, k_0 + 200$ straddling k_{true} and chose the model with minimum MSE.

IHT makes the cross-validation choice of model size straightforward. For cross-validation with LASSO and MCP, we used the cross-validation and response prediction routines in `glmnet` and `ncvreg`. To ensure roughly comparable lengths of regularization paths and therefore commensurate compute times, we capped the maximum permissible degrees of freedom at $k_{\text{true}} + 100$ for both LASSO and MCP regression routines. The case of MCP regression is peculiar since `ncvreg` does not cross-validate the γ parameter. We modified the approach of Breheny and Huang (Breheny and Huang, 2011) to obtain a suitable γ for each model. Their protocol entails cross-validating λ once with the default $\gamma = 3$ and checking if the optimal λ , which we call λ_{best} , exceeds the minimum lambda λ_{min} guaranteeing a convex penalty. Whenever $\lambda_{\text{best}} \leq \lambda_{\text{min}}$, we incremented γ by 1 and cross-validated λ again. We repeated this process until $\lambda_{\text{best}} > \lambda_{\text{min}}$. The larger final γ then became the default for the next simulation, thereby amortizing the selection of a proper value of γ across all 10 simulations for a given k_{true} . This procedure for selecting γ ensured model selection stability while simultaneously avoiding expensive cross-validation over a full grid of γ and λ values. The reported compute times for MCP reflect this procedure, though we never needed to increment γ in our simulations.

Table 1 shows the results of our simulation. The various columns of the table summarize true positive recovery, recovered model size, prediction error, and compute times for each model size k_{true} . In infor-

Model size	Penalty	True Pos Mean(SD)	Total Pos Mean(SD)	MSE Mean(SD)	Time Mean(SD)
100	IHT	94.7 (2.9)	96.6 (3.4)	0.006 (0.0001)	135.3 (6.9)
	LASSO	96.0 (2.6)	134.8 (7.5)	0.013 (0.0002)	59.0 (13.81)
	MCP	88.3 (3.2)	88.3 (3.2)	0.013 (0.0008)	186.3 (45.43)
200	IHT	190.3 (3.0)	191.2 (3.7)	0.006 (0.0003)	146.0 (6.3)
	LASSO	189.9 (2.3)	228.4 (8.1)	0.019 (0.0003)	63.2 (18.28)
	MCP	172.2 (5.0)	172.2 (5.0)	0.018 (0.0026)	185.9 (55.49)
300	IHT	283.1 (5.4)	284.4 (5.7)	0.007 (0.0001)	135.8 (9.2)
	LASSO	280.2 (4.5)	320.2 (5.5)	0.033 (0.0029)	50.1 (5.59)
	MCP	252.6 (17.0)	252.6 (17.0)	0.033 (0.0029)	137.5 (10.01)

Table 1: Model selection performance on NFBC1966 chromosome 1 data.

mation theoretic terms, LASSO exhibits excellent recall but suboptimal precision. MCP demonstrates suboptimal recall but optimal precision. IHT ameliorates the worst features of both LASSO and MCP. IHT recovers more true positives than MCP and fewer false positives than LASSO. Furthermore, IHT consistently attains the best prediction error on the validation set. Despite these benefits, the IHT pays only a modest price in computational speed versus LASSO; it is only 2-3x slower than LASSO, and it is fully competitive with MCP on this metric.

3.2 Speed comparisons

Our next numerical experiment highlights the sacrifice in computational speed incurred with compressed genotypes. The genotype matrix \mathbf{X}_{chr1} is now limited to patients with both BMI and directly observed weight, a condition imposed by Sabatti et al (2009). The response vector \mathbf{y} is the log body mass index (BMI) from NFBC1966. As mentioned previously, we included the SEXOCPG factor and the first two principal components as nongenetic covariates. We then ran three different configurations on a single compute node. The first used the floating point version of \mathbf{X}_{chr1} . We did not explicitly enable any multicore calculations. For the second run, we used a compressed copy of \mathbf{X}_{chr1} with multicore options enabled, but we disabled the GPU acceleration. The third run used the compressed \mathbf{X}_{chr1} data with both multicore and GPU acceleration. We ran each algorithm over a regularization path of model sizes $k = 5, 10, 15, \dots, 100$ and averaged compute times over 10 runs. For all uncompressed arrays, we used double precision arithmetic.

Table 2 shows the compute times. The floating point variant is clearly the fastest, requiring about 8 seconds to compute all models. The analysis using PLINK compression with a multicore CPU suffers a 17-fold slowdown, clearly demonstrating the deleterious effects on compute times resulting from repeated decompression and on-the-fly standardization. Enabling GPU acceleration leads to an 8x slowdown but fails to entirely bridge the performance gap suffered under compressed data. At this juncture, we make several remarks about GPU computing. First, the computational burden of analyzing just a single chromosome does not fully exploit GPU capabilities; hence, Table 2 does not demonstrate the full potential of GPU acceleration. Second, the value of GPU acceleration becomes more evident in crossvalidation: a 5-fold crossvalidation on one machine requires either five hexcore CPUs or one hexcore CPU and one GPU. The latter configuration lies within modern workstation capabilities. Third, our insistence on the use of double precision arithmetic dims the luster of GPU acceleration. Indeed, our experience is that using compressed arrays and a GPU with single precision arithmetic is only 1.7x slower than the corresponding floating point compute times. Furthermore, while we limit our computations to one CPU with six physical cores, including additional physical cores improves compute times even for

Data type	Mean Time	Standard Deviation
Uncompressed Data	8.27	0.056
Compressed Data, no GPU	141.28	0.998
Compressed Data with CPU + GPU	65.48	0.040

Table 2: Computational times in seconds on NFBC1966 chromosome 1 data.

Phenotype	n	p	Transform	m_{best}	Compute Time (Hours)
BMI	5122	333,656	log	2	1.12
HDL	4729	333,774	none	9	1.28
LDL	4715	333,771	none	6	1.32
TG	4728	333,769	log	10	1.49

Table 3: Dimensions of data used for each phenotype in GWAS experiment. Here n is the number of cases, p is the number of predictors (genetic + covariates), and m_{best} is the best cross-validated model size. Note that m_{best} includes nongenetic covariates.

compressed data without a GPU.

3.3 Application to lipid phenotypes

For our final numerical experiment, we embarked on a genome-wide search for associations based on the full $n \times p$ NFBC1966 genotype matrix X . In addition to BMI, this analysis considered three additional phenotypes from Sabatti et al. (2009): HDL cholesterol (HDL), LDL cholesterol (LDL), and triglycerides (TG). HDL, LDL, and TG all use SEXOCPG and the first two principal components as nongenetic covariates, but they also use BMI as a covariate. Quality control on SNPs included filters for minor allele frequencies below 0.01 and Hardy-Weinberg P -values below 10^{-5} . Subjects with unobserved or missing traits were excluded from analysis. We applied further exclusion criteria per Sabatti et al. (2009); for analysis with BMI, we excluded subjects without direct weight measurements, and for analysis of TG, HDL, and BMI, we excluded subjects with nonfasting blood samples and subjects on diabetes medication. These filters yield different values of n and p for each trait. Table 3 records problem dimensions and trait transforms.

We performed 5-fold cross-validation for the best model size over a path of sparsity levels $k = 1, 2, \dots, 50$. Refitting the best model size yielded the selected predictors and effect sizes. Table 3 records the compute times and best model sizes, while Table 4 shows the SNPs recovered by IHT.

One can immediately see that IHT does not collapse causative SNPs in strong linkage disequilibrium. IHT finds an adjacent pair of SNPs rs6917603 and rs9261256 for HDL. For TG, rs11974409 is one SNP separated from rs2286276, while SNP rs676210 is one SNP separated from rs673548. IHT does not flag rs673548 but its association with TG is known. Common sense suggests treating each associated pair as a single predictor.

Our analysis replicates several association from the literature but finds new ones as well. For example, Sabatti *et al.* found associations between TG and the SNPs rs1260326 and rs10096633, while rs2286276 was identified elsewhere. The SNPs rs676210, rs7743187, rs6917603, rs2000571, and rs3010965 are new associations with TG. We find that SNP rs6917603 is associated with all four traits; the BMI connection was missed by Sabatti *et al.*.

The association of SNP rs6917603 with BMI may be secondary to its association to lipid levels.

Phenotype	Chromosome	SNP	Position	β	Status
BMI	6	rs6917603	30125050	-0.01995	Unreported
HDL	6	rs6917603	30125050	0.10100	Reported Sabatti <i>et al.</i> (2009)
	6	rs9261256	30129920	-0.06252	Nearby
	11	rs7120118	47242866	-0.03351	Reported Sabatti <i>et al.</i> (2009)
	15	rs1532085	56470658	-0.04963	Reported Consortium (2013)
	16	rs3764261	55550825	-0.02808	Reported Sabatti <i>et al.</i> (2009)
	16	rs7499892	55564091	0.02625	Reported Surakka <i>et al.</i> (2012)
LDL	1	rs646776	109620053	0.09211	Reported Sabatti <i>et al.</i> (2009)
	2	rs693	21085700	-0.08544	Reported Sabatti <i>et al.</i> (2009)
	6	rs6917603	30125050	-0.07536	Reported Kettunen <i>et al.</i> (2012)
TG	2	rs676210	21085029	0.03633	Nearby
	2	rs1260326	27584444	-0.04088	Reported Sabatti <i>et al.</i> (2009)
	6	rs7743187	25136642	0.03450	Unreported
	6	rs6917603	30125050	-0.08215	Unreported
	7	rs2286276	72625290	0.01858	Reported Kim <i>et al.</i> (2011)
	7	rs11974409	72627326	0.01759	Nearby
	8	rs10096633	19875201	0.03781	Reported Sabatti <i>et al.</i> (2009)
	13	rs3010965	60937883	0.02828	Unreported
	19	rs2304130	19650528	0.03039	Reported Waterworth <i>et al.</i> (2010)

Table 4: Computational results from the GWAS experiment. Here β is the calculated effect size. Known associations include the relevant citation.

Indeed, a multivariate analysis of BMI, HDL, LDL, and TG reveals a stronger association of BMI to rs6917603 ($P = 9.88 \times 10^{-105}$) with a higher F -score ($F = 129.067$) than a univariate analysis of BMI alone ($P = 1.19 \times 10^{-15}$, $F = 64.533$). The four traits exhibit correlation coefficients ρ with magnitudes between 0.25 and 0.35. Thus, the pleiotropic effect of rs6917603 on the traits is not surprising. A more extensive analysis that incorporates nearby genetic markers in LD may further improve evidence of association to these correlated traits (Fan *et al.*, 2013, 2015; Wang *et al.*, 2015). A similar argument applies to SNP rs676210; it is very close to rs673548 and is strongly associated with oxidative LDL cholesterol (Mäkelä *et al.*, 2013), so the association is likely a consequence of pleiotropy.

IHT flags an association between SNP rs2304130 and TG. This association was validated in a large meta-analysis of 3,540 cases and 15,657 controls performed after (Sabatti *et al.*, 2009) was published. Some of the effect sizes in Table 4 are difficult to interpret. For example, IHT estimates effects for rs10096633 ($\beta = 0.03781$) and rs1260326 ($\beta = -0.04088$) that are both smaller and in opposite sign to the estimates in (Sabatti *et al.*, 2009).

The potential new associations to TG with SNPs rs7743187 and rs3010965 are absent from the literature. Furthermore, our analysis misses borderline significant associations identified by Sabatti *et al.* (2009), such as rs2624265 for TG and rs9891572 for HDL; these SNPs were never flagged in later studies. In this regard it is worth emphasizing that the best model size k_{best} delivered by cross-validation is a guide rather than definitive truth. Figure 1 shows that the difference in MSE between k_{best} and adjacent model sizes can be quite small. Models of a few SNPs more or less than k_{best} predict trait values about as well. Thus, TG with $k_{\text{true}} = 10$ has MSE = 0.2310, while TG $k_{\text{true}} = 4$ has MSE = 0.2315. Indeed, refitting the TG phenotype with $k = 4$ yields only three significant SNPs: rs1260326, rs6917603, and rs10096633. The SNPs rs7743187 and rs3010965 are absent from this model, so we should be

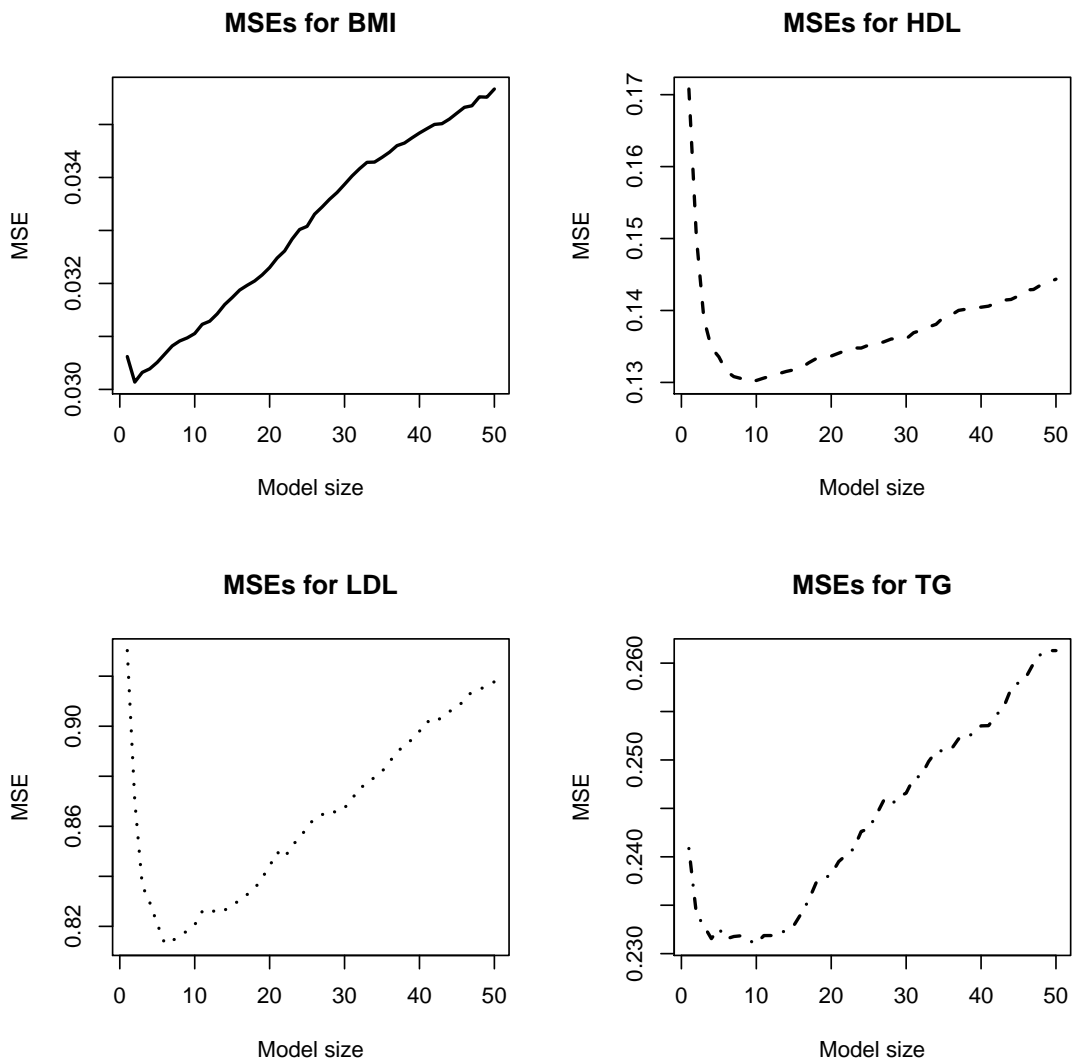


Figure 1: Mean squared error as a function of model size, as averaged over 5 cross-validation slices, for four lipid phenotypes from NFBC 1966.

cautious in declaring new associations. This example also highlights the great value in computing many model sizes, which univariate regression schemes typically fail to do.

Finally, we comment on compute times. IHT requires about 1.5 hours to cross-validate the best model size over 50 possible models using double precision arithmetic. Obviously, computing fewer models can decrease this compute time substantially. If the phenotype in question is scaled correctly, then analysis with IHT may be feasible with single precision arithmetic, which yields an additional speedup as suggested in Section 3.2. Analyses requiring better accuracy will benefit from the addition of double precision registers in newer GPU models. Thus, our analysis still retains room for speedup without sacrificing model selection performance if compute speed is a key concern.

4 Discussion

The current paper demonstrate the utility of iterative hard thresholding (IHT) in large-scale GWAS analysis. Despite its nonconvex nature, the IHT algorithm enjoys provable convergence guarantees under certain regularity conditions. Its model selection performance exceeds that of more popular and mature tools such as LASSO- and MCP-regression. Our software directly and intelligently handles the compression protocol widely used to store GWAS genotypes. Finally, IHT can be accelerated by exploiting shared-memory and massively parallel processing hardware. As a rule of thumb, computation times with IHT may scale as $\mathcal{O}(np)$ or somewhat worse if more predictors with small effect sizes come into play.

Our implementation addressed a gap in current software packages for GWAS analysis. Lack of general support for PLINK binary genotype data, poor memory management, and limited parallel capabilities discourage use of software such as `glmnet` or `ncvreg`. Our IHT package enables analysis of models of any sparsity, while `gpu-lasso` is designed solely for very sparse models. It also cross-validates for the best model size over a range of possible models. Given the importance of cross-validation, `IHT.jl` provides a useful tool for GWAS.

It is worth noting that IHT is hardly a panacea for GWAS. Analysts must still deal with perennial statistical issues such as correlated predictors and sufficient sample sizes. Furthermore, while the estimation properties of hard thresholding algorithms are well understood, IHT lacks a coherent theory of inference for assessing statistical significance. In contrast, considerable progress has been made in understanding postselection inference with LASSO penalties (Lockhart *et al.*, 2014; Taylor and Tibshirani, 2015; Lee *et al.*, 2016).

Our analysis framework also neglects the wealth of data available from whole genome sequencing. As sketched in Section 2.1, the mutual coherence condition for convergence of IHT discourages the use of IHT on strongly correlated predictors such as those that arise from analyzing genome sequences base-by-base. Users interested in rare variant analysis could feasibly use IHT to their advantage by lumping correlated rare SNPs into a single predictor and then running penalized regression on these measures of genetic burden. In principle, one could combine burden predictors with polymorphic SNP predictors.

As formulated here, the scope of application for IHT is limited to linear least squares regression. Researchers have begun to extend IHT to generalized linear models, particularly logistic regression (Bahmani *et al.*, 2013; Yuan *et al.*, 2014). We anticipate that IHT will eventually join LASSO and MCP in the standard toolbox for sparse linear regression. In our opinion, gene mapping efforts clearly stand to benefit from this advance.

Acknowledgements

The authors are grateful to Aditya Ramdas for his guidance on IHT and to Dennis Sun for discussions about general model selection. We benefitted from discussions about IHT at the American Institute of Mathematics. Finally, we thank the Stanford University Statistics Department for hosting us as sabbatical guests during the 2014-2015 academic year.

Funding

This work was supported by grants from the National Human Genome Research Institute [HG006139] and the National Institute of General Medical Sciences [GM053275] to K.L. and fellowship support from the National Human Genome Research Institute [HG002536] and the National Science Foundation [DGE-0707424] to K.L.K.

References

- Abraham, G., Kowalczyk, A., Zobel, J., and Inouye, M. (2012). SparSNP: Fast and memory-efficient analysis of all SNPs for phenotype prediction. *BMC Bioinformatics*, **13**(1), 88.
- Agarwal, A., Negahban, S., and Wainwright, M. J. (2012). Fast global convergence rates of gradient methods for high-dimensional statistical recovery. *The Annals of Statistics*, **40**(5), 2452–2482.
- Ayers, K. and Lange, K. (2008). Penalized estimation of haplotype frequencies. *Bioinformatics*, **24**, 1596–1602.
- Bahmani, S., Raj, B., and Boufounos, P. T. (2013). Greedy sparsity-constrained optimization. *Journal of Machine Learning Research*, **14**(3), 807–841.
- Beck, A. and Teboulle, M. (2009). A fast iterative shrinkage thresholding algorithm for linear inverse problems. *SIAM Journal of Imaging Sciences*, **2**(1), 183–202.
- Blumensath, T. (2012). Accelerated iterative hard thresholding. *Signal Processing*, **2**(1), 183–202.
- Blumensath, T. and Davies, M. E. (2008). Iterative hard thresholding for sparse approximation. *Journal of Fourier Analysis and Applications*, **14**, 629–654.
- Blumensath, T. and Davies, M. E. (2009). Iterative hard thresholding for compressed sensing. *Applications of Computational and Harmonic Analysis*, **27**, 265–274.
- Blumensath, T. and Davies, M. E. (2010). Normalized iterative hard thresholding: Guaranteed stability and performance. *IEEE Journal of Selected Topics in Signal Processing*, **4**(2), 298–309.
- Breheny, P. and Huang, J. (2011). Coordinate descent algorithms for nonconvex penalized regression, with applications to biological feature selection. *Annals of Applied Statistics*, **5**(1), 232–253.
- Candés, E., Romberg, J. K., and Tao, T. (2006). Stable signal recovery from incomplete and inaccurate measurements. *Communications on Pure and Applied Mathematics*, **59**(8), 1207–1223.
- Chang, C. C., Chow, C. C., Tellier, L. C., Vattikuti, S., Purcell, S. M., and Lee, J. J. (2015). Second-generation PLINK: rising to the challenge of larger and richer datasets. *GigaScience*, **4**(7).
- Chen, G. K. (2012). A scalable and portable framework for massively parallel variable selection in genetic association studies. *Bioinformatics*, **28**, 719–720.
- Consortium, G. L. G. (2013). Discovery and refinement of loci associated with lipid levels. *Nature Genetics*, **45**, 1274–1283.
- Dai, W. and Milenkovic, O. (2009). Subspace pursuit for compressive sensing signal reconstruction. *IEEE Transactions on Information Theory*, **55**(5), 2230–2249.
- Dobson, A. J. and Barnett, A. G. (2008). *An Introduction to Generalized Linear Models*, volume 3. Chapman and Hall/CRC Press.

- Efron, B., Hastie, T., Johnstone, I., and Tibshirani, R. (2004). Least angle regression. *The Annals of Statistics*, **32**(2), 407–499.
- Fan, R., Wang, Y., Mills, J. L., Wilson, A. F., Bailey-Wilson, J. E., and Xiong, M. (2013). Functional linear models for association analysis of quantitative traits. *Genetic epidemiology*, **37**(7), 726–742.
- Fan, R., Wang, Y., Boehnke, M., Chen, W., Li, Y., Ren, H., Lobach, I., and Xiong, M. (2015). Gene level meta-analysis of quantitative traits by functional linear models. *Genetics*, **200**, 1089–115.
- Foucart, S. (2011). Hard thresholding pursuit: An algorithm for compressive sensing. *SIAM Journal on Numerical Analysis*, **49**(6), 2543–2563.
- Friedman, J., Hastie, T., Höfling, H., and Tibshirani, R. (2007). Pathwise coordinate optimization. *Annals of Applied Statistics*, **1**(2), 302–332.
- Friedman, J., Hastie, T., and Tibshirani, R. (2010). Regularization paths for generalized linear models via coordinate descent. *Journal of Statistical Software*, **33**(1), 1–22.
- Golub, G., Klema, V., and Stewart, G. W. (1976). Rank degeneracy and least squares problems. Technical report, Stanford University Department of Computer Science.
- Hastie, T., Friedman, J., and Tibshirani, R. (2009). *The Elements of Statistical Learning*, volume 2. Springer.
- Jain, P., Tewari, A., and Kar, P. (2014). On iterative hard thresholding methods for high-dimensional m-estimation. In *Advances in Neural Information Processing Systems*, pages 685–693.
- Jiang, D. and Huang, J. (2011). Majorization minimization by coordinate descent for concave penalized generalized linear models. Technical Report 412, Department of Statistics and Actuarial Science, The University of Iowa.
- Kettunen, J., Tukiainen, T., Sarin, A.-P., Ortega-Alonso, A., *et al.* (2012). Genome-wide association study identifies multiple loci influencing human serum metabolite levels. *Nature Genetics*, **44**, 269–276.
- Kim, Y. J., Go, M. J., Hu, C., Hong, C. B., *et al.* (2011). Large-scale genome-wide association studies in east asians identify new genetic loci influencing metabolic traits. *Nature Genetics*, **43**(10), 990–995.
- Lange, K. (2010). *Numerical Analysis for Statisticians*. Springer Science & Business Media.
- Lange, K., Papp, J. C., Sinsheimer, J. S., Sripracha, R., Zhou, H., and Sobel, E. M. (2013). Mendel: The Swiss army knife of genetic analysis programs. *Bioinformatics*, **29**, 1568–1570.
- Lange, K., Papp, J. C., Sinsheimer, J. S., and Sobel, E. M. (2014). Next generation statistical genetics: Modeling, penalization, and optimization in high-dimensional data. *Annual Review of Statistics and Its Application*, **1**(1), 279–300.
- Lee, J. D., Sun, D. L., Sun, Y., and Taylor, J. E. (2016). Exact post-selection inference, with application to the lasso. *The Annals of Statistics*, **44**(3), 907–927.
- Lockhart, R., Taylor, J., Tibshirani, R. J., and Tibshirani, R. (2014). A significance test for the lasso. *The Annals of Statistics*, **42**(2), 413–468.
- Loh, P.-L. and Wainwright, M. J. (2013). Regularized m-estimators with nonconvexity: Statistical and algorithmic theory for local optima. In *Advances in Neural Information Processing Systems*, pages 476–484.

- Mäkelä, K., Seppälä, I., Hernesniemi, J., Lyytikäinen, L., *et al.* (2013). Genome-wide association study pinpoints a new functional apolipoprotein b variant influencing oxidized low-density lipoprotein levels but not cardiovascular events: Atheroremo consortium. *Cardiovascular Genetics*, **6**, 73 – 81.
- Mallat, S. and Zhang, Z. (1993). Matching pursuits with time-frequency dictionaries. *SIAM Journal on Computing*, **24**(2), 3397–3415.
- Natarajan, B. K. (1995). Sparse approximate solutions to linear systems. *SIAM Journal on Computing*, **24**(2), 227–234.
- Needell, D. and Tropp, J. A. (2009). CoSaMP: iterative signal recovery from incomplete and inaccurate samples. *Applied and Computational Harmonic Analysis*, **26**(3), 301–321.
- Purcell, S., Neale, B., Todd-Brown, K., Thomas, L., *et al.* (2007). PLINK: A tool set for whole-genome association and population-based linkage analyses. *American Journal of Human Genetics*, **81**(3), 559–575.
- Sabatti, C., Service, S. K., Hartikainen, A.-L., Pouta, A., Ripatti, S., Brodsky, J., *et al.* (2009). Genome-wide association analysis of metabolic traits in a birth cohort from a founder population. *Nature Genetics*, **41**(1), 35–46.
- Surakka, I., Whitfield, J. B., Perola, M., Visscher, P. M., *et al.* (2012). A genome-wide association study of monozygotic twin-pairs suggests a locus related to variability of serum high-density lipoprotein cholesterol. *Twin Research and Human Genetics*, **15**, 691–699.
- Taylor, J. and Tibshirani, R. J. (2015). Statistical learning and selective inference. *Proceedings of the National Academy of Sciences*, **112**(25), 7629–7634.
- Tibshirani, R. (1996). Regression shrinkage and selection via the lasso. *Journal of the Royal Statistical Society, Series B*, **58**(1), 267–288.
- Tropp, J. A. (2006). Just relax: Convex programming methods for identifying sparse signals in noise. *IEEE Transactions on Information Theory*, **52**(3), 1030–1051.
- Tropp, J. A. and Gilbert, A. C. (2007). Signal recovery from random measurements via orthogonal matching pursuit. *IEEE Transactions on Information Theory*, **53**(12), 4655–4666.
- Wang, Y., Liu, A., Mills, J. L., Boehnke, M., Wilson, A. F., Bailey-Wilson, J. E., Xiong, M., Wu, C. O., and Fan, R. (2015). Pleiotropy analysis of quantitative traits at gene level by multivariate functional linear models. *Genetic epidemiology*, **39**(4), 259–275.
- Waterworth, D. M., Ricketts, S. L., Song, K., Chen, L., *et al.* (2010). Genetic variants influencing circulating lipid levels and risk of coronary artery disease. *Arteriosclerosis, Thrombosis, and Vascular Biology*, **30**, 2264–2276.
- Wu, T. T. and Lange, K. (2008). Coordinate descent algorithms for lasso penalized regression. *Annals of Applied Statistics*, **2**(1), 224–244.
- Wu, T. T., Chen, Y. F., Hastie, T., Sobel, E., and Lange, K. (2009). Genome-wide association analysis by lasso penalized logistic regression. *Bioinformatics*, **25**(6), 714–721.
- Yang, J., Benyamin, B., McEvoy, B. P., Gordon, S., *et al.* (2010). Common SNPs explain a large proportion of the heritability for human height. *Nature Genetics*, **42**(7), 565–569.
- Yuan, X., Li, P., and Zhang, T. (2014). Gradient hard thresholding pursuit for sparsity-constrained optimization. *Journal of Machine Learning Research*, **32**.

Zhang, C.-H. (2010). Nearly unbiased variable selection under minimax concave penalty. *Annals of Statistics*, **38**(2), 894–942.